

## Preparation of polypyrrole/Poly(N-methylpyrrole)/nano-ZnO Composite and Its Anticorrosive Performance

Falong Wang<sup>1</sup>, Yansheng Zheng<sup>1,2,\*</sup>, Chunyan Mo<sup>1</sup>, Chuanbo Hu<sup>1</sup>, Qian Mo<sup>1</sup>

<sup>1</sup> School of Biological and Chemical Engineering, Guangxi University of Science and Technology, Liuzhou 545006, Guangxi China

<sup>2</sup> Lushan College of Guangxi University of Science and Technology, Liuzhou 545616, Guangxi China

\*E-mail: [barry181@yeah.net](mailto:barry181@yeah.net)

Received: 14 May 2015 / Accepted: 7 June 2015 / Published: 24 June 2015

---

In the presence of iron trichloride as oxidant and the p-toluenesulfonic acid as dopant, the polypyrrole/poly(N-methylpyrrole)/nano-ZnO, the polypyrrole/nano-ZnO, the polypyrrole/poly(N-methylpyrrole), the poly(N-methylpyrrole) and polypyrrole composites were prepared. The morphology and structure of composite was characterized by scanning electron microscopy, X-ray pattern, UV-vis and FT-IR spectra. The carbon steel was coated polyurethane with respectively adding five kinds of composites as filler, and was soaked in mass fraction of 3.5% NaCl solution, the anticorrosive performance of coating was researched with the Open Circuit Potential, the Polarization Curve, the Electrochemical Impedance Spectroscopy and the immersion test. The results show that the anticorrosive performance of the polyurethane/polypyrrole/poly(N-methylpyrrole)/nano-ZnO hybrid coating was optimum, in that the open circuit potential values was maximum, the corrosion current densities and rate was minimum.

---

**Keywords:** conductive polymer; polypyrrole; anticorrosive performance; electrochemical; coating.

### 1. INTRODUCTION

Metal corrosion is a serious problem throughout the world, it not only causes the waste of energy and resources, but also is harmful to human health [1-2]. Hence, developing the new anticorrosion coating with economy, high performance and pollution free has become a new trend of anticorrosion field [3]. As the novel macromolecules materials, conducting polymers have attracted many people's attention. The conducting polymers have been widely studied because of the specific properties. Among these conducting polymers, the polypyrrole(PPY) dues to the environmental stability, superior electric conductivity and easily synthesized [4-7], has been widely applied in various

aspects such as photodiodes, sensors, batteries, and technological membranes [8-11]. The studies have found that the coating containing PPY can prevent metals from corrosion. Further it has been shown that the PPY coating can limit the metal corrosion in the membrane layer interface, which is result from the information of passive layer between steel surface and coating [12].

Although the PPY coating has the good protection of metals, the interfacial adhesion between the coating and metal substrate is poor due to the dissimilarity of physical and chemical structures, which may affect the anticorrosion performance [13-15]. Consequently, many methods have been developed to improve the adhesion and anticorrosion performance. Duran [16] found that PPY derivatives such as Poly(N-methylpyrrole)(PNY) has been considered as organic inhibitors that can improve the corrosion rate. Further it has been found that the increase of monomer in molecular chain can improve the adhesion. So, it can consider the compound PPY and PNY. The inorganic nanoparticles such as nano-zinc-oxide(nano-ZnO) have better corrosion protection abilities, which posses high strength, chemical stability and anticorrosion performance. Mostafaei [17] found that the coating containing the nano-ZnO can effectively improve the corrosion resistance.

In this study, the composite of polypyrrole/poly(N-methylpyrrole)/nano-ZnO, the polypyrrole/nano-ZnO, the polypyrrole/poly(N-methylpyrrole), the poly(N-methylpyrrole) and polypyrrole were prepared. The polyurethane respectively adding compsite as filler, coated the steel surfaces. The composites were characterized by scanning electron microscopy(SEM), X-ray pattern, UV-vis and FT-IR spectra. The coating was studied with electrochemical measurements and immersion test in 3.5% NaCl solution.

## 2. EXPERIMENTAL

### 2.1 Materials

In this study, all chemical reagents were analytical laboratory grade, which obtained from different sources. Pyrrole and N-methylpyrrole were distilled before use, and all other chemical reagents used without any further purification. Pyrrole was obtained from Shanghai SaiEn chemical technology Co., Ltd. N-methylpyrrole was purchased from Chengdu chemical Co., Ltd.

Iron chloride( $\text{FeCl}_3$ ) was purchased from Taishang Gangdong Overseas reagent plastic Co., Ltd. p-toluenesulfonic acid(TsOH) was obtained from Tianjin Kemiou Chemical reagent Co., Ltd. Sodium chloride(NaCl), acetone were obtained from Xilong Chemical Co., Ltd. Methanol was purchased from Guangzhou Chemical reagent Co., Ltd. Ethanol was obtained from Chengdu Kelong Chemical reagent Co., Ltd. Polyurethane(PU), Polyurethane-curing agent were Foushang Ouqi coating Co., Ltd. Nano-ZnO with particle size of 50 nm was obtained from Tianjin ZhiYuan chemical Co., Ltd.

### 2.2 Preparation of Polypyrrole/Poly(N-methylpyrrole)/ZnO composite

Polypyrrole/Poly(N-methylpyrrole)/ZnO(PNZO) was prepared by the situ polymerization method, Pyrrole and N-methylpyrrole were distilled to colorless before usage. For this preparation, the

7.41 ml of N-methylpyrrole and the 6.92 ml of pyrrole mixed, and 50 ml of distilled water was added into. The mixture that 12.9 g of p-toluenesulfonic acid and 50 ml of distilled water were added to the above solution, and 3.77 g of Nano-ZnO was dispersed by the ultrasound in mixed solution, then it was added to the three mouth flask, magnetic stirring for 40 min. 8.11 g of FeCl<sub>3</sub> was dissolved in 50 ml of distilled water, then it was slowly added to the above mixture solution under mechanically stirring in an ice bath, the temperature less than 0 °C was maintained for 5 hours to complete the preparation. Then mixture solution was filtered and washed several times with methanol and distilled water. Eventually, the cake was dried at 60 °C for 12 hours in air oven to obtain dark powder-Polypyrrole/Poly(N-methylpyrrole)/ZnO(PPZO). In the same way, pure Polypyrrole(PPY) and Poly(N-methylpyrrole)(PNY), Polypyrrole/Poly(N-methylpyrrole)(PPN) were prepared without nano-ZnO, and Polypyrrole/ZnO(PZO) were prepared.

### 2.3 Preparation of hybrid coatings

The steel samples with 25 mm×12 mm dimensions were used in film-base. To clear the existing passive layer and obtain the smooth surface, the steel samples were mechanically polished by the 320 and 600 grade emery papers respectively, and degreased by ultrasound in ethanol and acetone, then air-dried at room temperature before usage. As the only fillers 0.1 g of PPZO was dispersed in 5.0 g of polyurethane and 10.0 g of polyurethane-curing agent system by ultrasound, and the hybrid coating of PPZO/PU was prepared. In the same way, the hybrid coating of PPy/PU, PNY/PU, PPN/PU, PZO/PU and pure PU coating were prepared. The five steel samples were respectively coated with the five hybrid coatings, and dried at 60 °C for 12 hours. The thickness of the coating was 100±5 μm. Fig. 1 shows the schematic preparation of PPZO/PU hybrid coating.

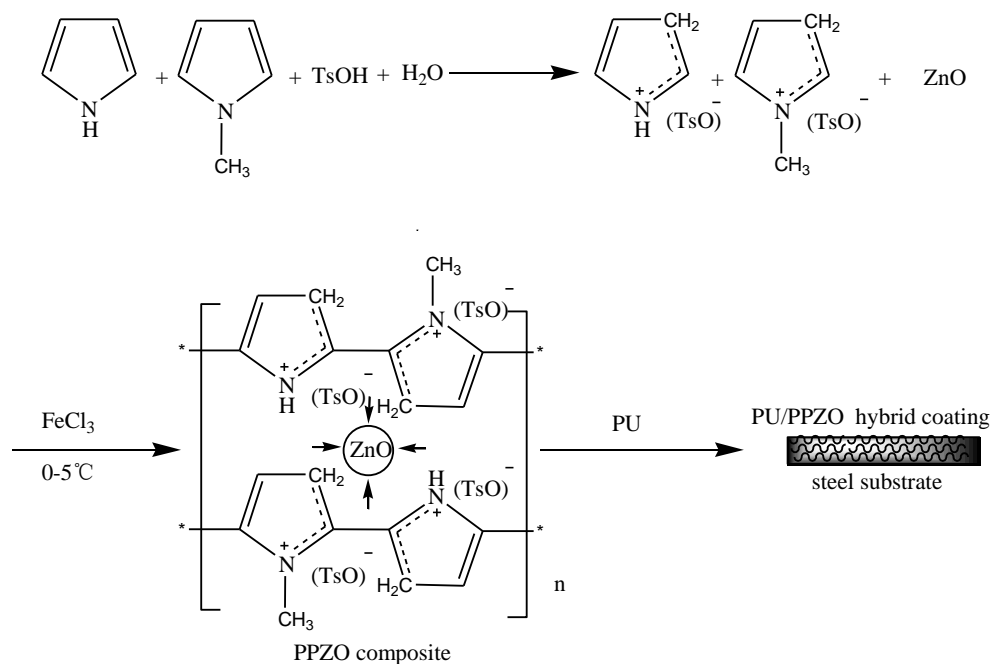


**Figure 1.** The schematic preparation of PU/PPZO hybrid coating

## 2.4 Characterization of composite

The scanning electron microscopy images of the samples were recorded using the S-3400N digital scanning electron microscopy. The XRD pattern of the samples were recorded using the DX-2700 X-ray diffraction in the range of  $10^{\circ}$ - $90^{\circ}$ . The UV-vis spectra of the samples were recorded using the UV-2102 PC spectrophotometer in the range of 190-240 nm, and the samples were prepared by dissolving in distilled water. The FI-IR spectra of the samples were recorded using the Nicolet 380 spectrometer by the KBr pellet technique in the range of  $4000$ - $500\text{ cm}^{-1}$ .

## 2.5 Evaluation of antirosion performance of the hybrid coatings

The anticorrosion performance of different coating was using the CHI66D electrochemical analyzer in 3.5% NaCl solution. The Open Circuit Potential(OCP), the Polarization Curve and the Electrochemical Impedance Spectroscopy(EIS) were recorded using the three-electrode electrochemical system with saturate calomel electrode as reference electrode, platinum gauze as a counter electrode and the steel samples as working electrode. The actually corrosion resistance of coating was researched by the immersion test, the different coating in 3.5% NaCl solution took the picture.

# 3. RESULTS AND DISCUSSION

## 3.1 Characterization of Composite

### 3.1.1 SEM Analysis

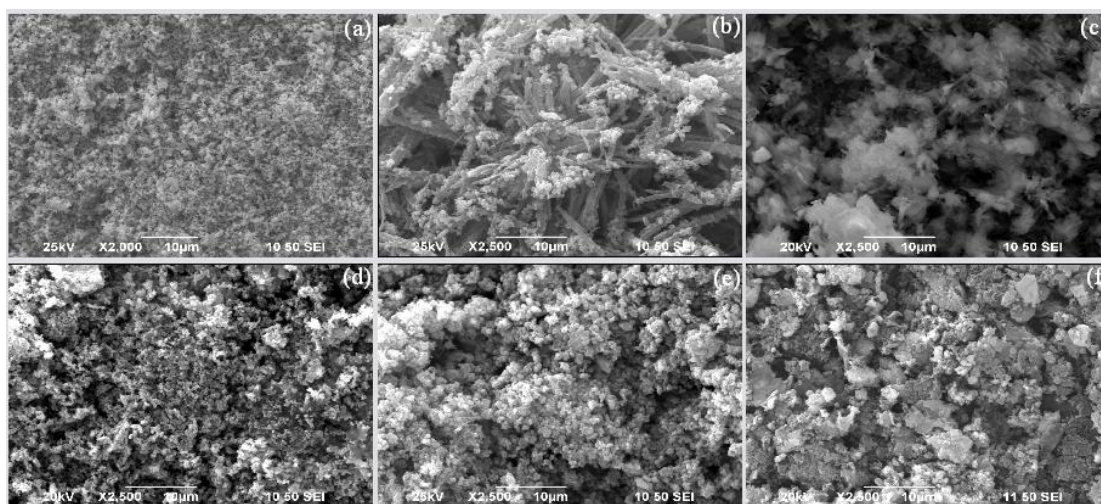
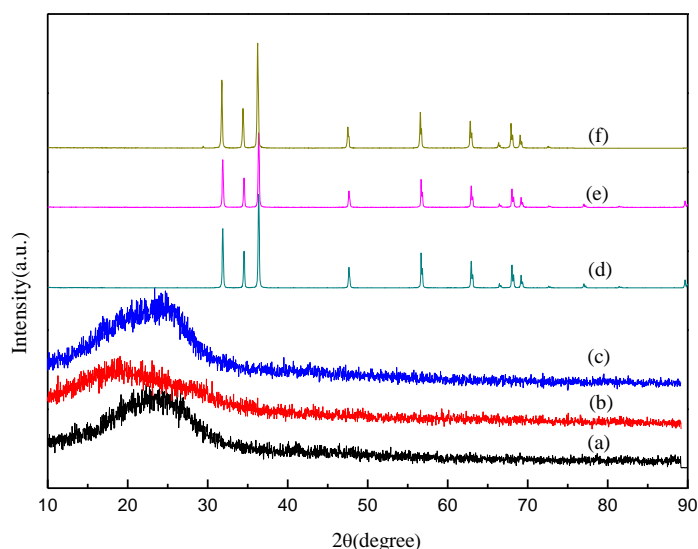


**Figure 2.** the SEM images of (a) nano-ZnO, (b) PPY, (c) PNY, (d)PPN, (e)PZO and (f)PPZO powders

Fig. 2 shows the SEM images of nano-ZnO, PPY, PNY, PPN, PZO and PPZO. It can be seen that the granular materials of nano-ZnO formed into agglomerations, whereas PPY containing the

flocculent materials formed into irregular structure. PNY is composed of irregular cloud-shape, and it has an obvious gap. PPN is closely connected of tiny particles, the density is better. When nano-ZnO was dispersed in the reaction system acting as the reaction cores, the deposition of monomer occurred on the surface of nano-ZnO particles. From Fig. 2, it can be seen that nano-ZnO particles of PZO and PPZO were fully covered with molecules [18]. It has been encapsulated into the polymer pores and makes significant improvement in its densification structure.

### 3.1.2 XRD characterization



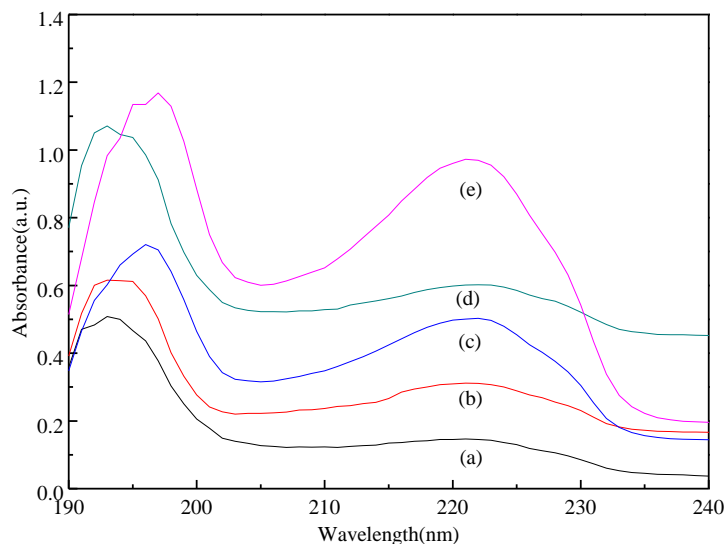
**Figure 3.** the XRD pattern of (a) nano-ZnO, (b) PPY, (c) PNY, (d) PPN, (e) PZO and (f) PPZO powders

Fig. 3 shows the XRD pattern of nano-ZnO, PPY, PNY, PPN, PZO and PPZO. It can be seen that broad diffraction peaks of PPY occur between  $16^\circ$  and  $28^\circ$  due to the parallel and perpendicular periodicity of the PPY chain [19]. The diffraction peaks of PNY at  $15^\circ$  and  $22^\circ$  may be due to the effective of the existence of the methyl substituent on the regularity of the whole polymer. The diffraction peaks of PPN are similar to PPY, yet they are wider and stronger, which is attributed to augment of monomer chain. From Fig. 3, the peaks of PZO and PPZO are very much similar to nano-ZnO. It implies that polymer has no effect on crystallization performance of nano-ZnO. Nevertheless, the diffraction peaks of polymer are disappeared, which is the existence of nano-ZnO.

### 3.1.3 UV-vis characterization

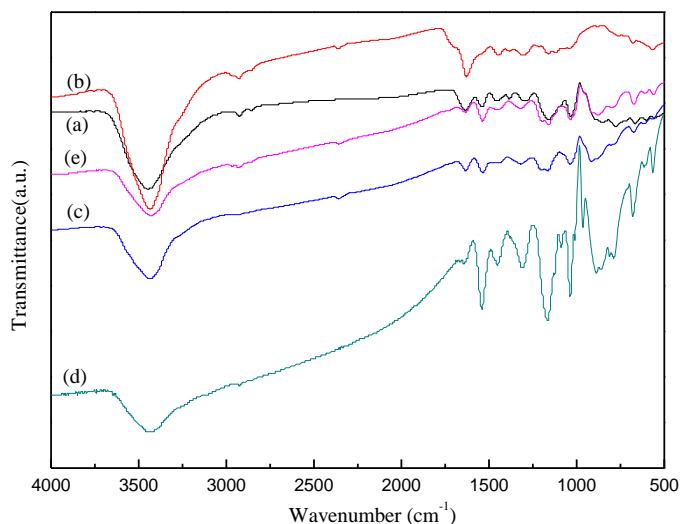
Fig. 4 shows the UV-vis spectra of PPY, PNY, PPN, PZO and PPZO, it is observed that PPY has two characteristic absorption peaks at 193 nm and 221 nm. The peaks at around 193 nm is assigned to  $n-\sigma^*$  transition of carbon and nitrogen atoms, while the peaks at around 221 nm is attributed to  $\pi-\pi^*$  transition of benzenoid to p-toluenesulfonic acid [20]. From Fig. 4, it has been found that the shapes of UV-vis spectra of PNY, PPN, PZO, PPZO are similar to PPY. When it contained the PNY, the

absorption peaks was red shifted and increased intensity. The change is due to the interaction between  $\pi$  electronics of pyrrole ring and C-H  $\sigma$ -bonds of methyl.



**Figure 4.** the UV-vis spectra of (a) PPY, (b) PNY, (c) PPN, (d) PZO and (e) PPZO powders

### 3.1.4 FT-IR characterization



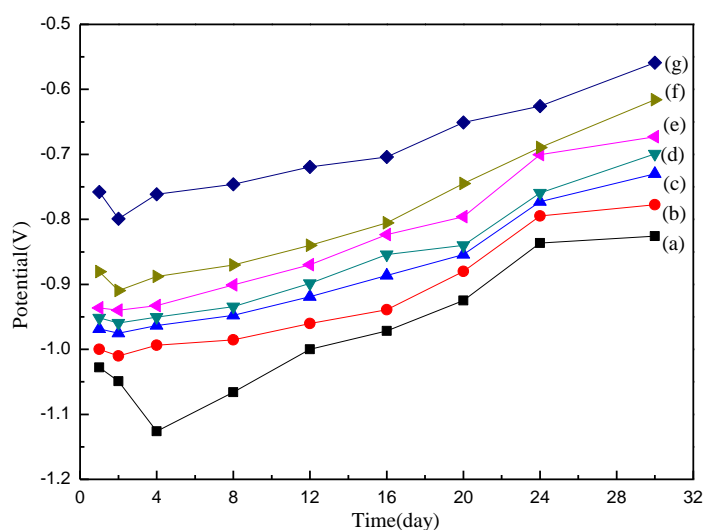
**Figure 5.** the FT-IR spectra of (a) PPY, (b) PNY, (c) PPN, (d) PZO and (e) PPZO powders

Fig. 5 show the FT-IR spectra of PPY, PNY, PPN, PZO and PPZO. We can be clearly seen that the FT-IR characteristic peaks of PPY are consistent with the literatures. The peak at  $3454\text{ cm}^{-1}$  is attributed to the N-H stretching of pyrrole ring and O-H stretching of p-toluenesulfonic acid [21]. The peak at  $1637\text{ cm}^{-1}$  is attributed to the C=C stretching of pyrrole ring and benzenoid ring. The peak at  $1165\text{ cm}^{-1}$  is attributed sulfo stretching of p-toluenesulfonic acid. The peak at  $1033\text{ cm}^{-1}$  and  $775\text{ cm}^{-1}$

are respectively to the C-H plane stretching vibration and out plane stretching bending. The characteristic peak of PNY is similar to PPY, yet it shows the absorption peaks of N-CH<sub>3</sub>. The characteristic peak of PPN is similar to PPY and PNY. When it contained the nano-ZnO, it produces the peak at 500<sup>-1</sup>-600 cm<sup>-1</sup>. The peak of PZO and PPZO shows that all the characteristic absorption peaks of PPY and PNY are present and the peaks compared with that of pure PPY and PNY are found to be shifted to lower wave number, it may be due to the incorporation of nano-ZnO into the polymer matrix causing certain physicochemical interaction existed between polymer and nano-ZnO particles.

### 3.2 Corrosion resistance of the coatings

#### 3.2.1 OCP studies



**Figure 6.** The OCP curves of (a) uncoated steel, (b) pure PU coating, the hybrid coating of (c) PU/PPY, (d) PU/PNY, (e) PU/PPN, (f) PU/PZP and (g) PU/PPZO

Fig. 6 shows the OCP variation values of uncoated steel, pure PU coating, the hybrid coating of PU/PPY, PU/PNY, PU/PPN, PU/PZP and PU/PPZO with the immersion time changes in 3.5% NaCl solution. During initial period, the OCP values of all samples are shifted to be shifted to negative direction, and then revert back to positive direction. The OCP values of the PU/PPZO hybrid coating were more positive than the other coatings, and the second is the PU/PZP coating. It indicates that the existent of nano-ZnO particles can improve the barrier properties of the composite coating [22]. From Fig. 6, the OCP values of the PU/PPN hybrid coatings was more positive than the PU/PPY and PU/PNY hybrid coatings, which indicated that the increase of polymer monomer can also enhance the anticorrosive performance [23-24]. The OCP variation values of PU/PPZO hybrid coating explained that the PPZO fillers can effectively improve the anticorrosive performance of PU in 3.5% NaCl solution.

3.2.2 Polarization Curve studies

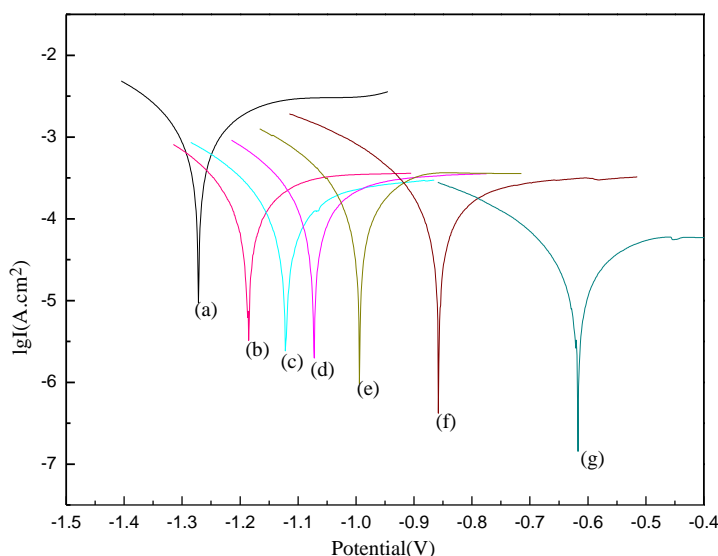


**Figure 7.** The Polarization Curve of (a) uncoated steel, (b) pure PU coating, the hybrid coating of (c) PU/PPY, (d) PU/PNY, (e) PU/PPN, (f) PU/PZP and (g) PU/PPZO

**Table 1.** The corrosion potential( $E_{corr}$ ), corrosion current density( $I_{corr}$ ) and corrosion rate( $V_{corr}$ ) values of uncoated and coated steel coupons in 3.5% NaCl solution

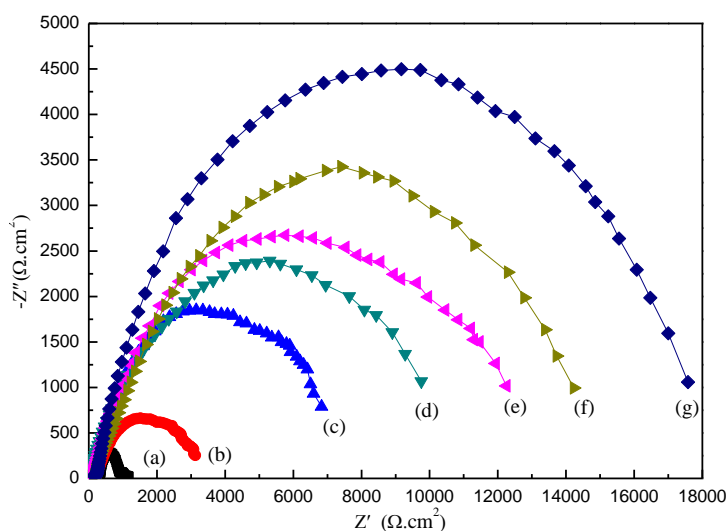
Coating	$E_{corr}/V$	$I_{corr}/(A/cm^2)$	$V_{corr}/(mm/a)$	$\beta_a(v/dec)$	$\beta_c(v/dec)$
Uncoated steel	-1.26	$7.24 \times 10^{-4}$	8.47	0.18	0.13
PU	-1.18	$1.20 \times 10^{-4}$	1.40	0.20	0.13
PU/PPY	-1.10	$6.76 \times 10^{-5}$	$7.91 \times 10^{-1}$	0.24	0.14
PU/PNY	-1.06	$5.62 \times 10^{-5}$	$6.58 \times 10^{-1}$	0.22	0.14
PU/PPN	-0.99	$3.39 \times 10^{-5}$	$3.97 \times 10^{-1}$	0.20	0.15
PU/PZP	-0.84	$2.30 \times 10^{-5}$	$2.69 \times 10^{-1}$	0.24	0.14
PU/PPZO	-0.61	$6.12 \times 10^{-6}$	$7.16 \times 10^{-2}$	0.23	0.18

Fig. 7 shows the Polarization Curve of uncoated steel, pure PU coating, the hybrid coating of PU/PPY, PU/PNY, PU/PPN, PU/PZP and PU/PPZO in 3.5% NaCl solution. Tab. 1 shows the corrosion potential( $E_{corr}$ ), the corrosion current density( $I_{corr}$ ), the corrosion rate( $V_{corr}$ ), anodic tafel slopes( $\beta_a$ ) and cathodic tafel slopes( $\beta_c$ ) values calculated based on the tafel line extrapolation method [25]. It can be seen that the anticorrosive performance of PU, PU/PPY, PU/PNY, PU/PPN, PU/PZP and PU/PPZO coating obviously enhance, when compared with the uncoated steel. The  $E_{corr}$  and  $I_{corr}$  values of uncoated steel were  $-1.26 V$  and  $7.24 \times 10^{-4} A/cm^2$  respectively. The  $E_{corr}$  values of the PU coating increased to  $-1.10 V$ , the  $I_{corr}$  values decreased to  $1.20 \times 10^{-4} A/cm^2$ . The  $E_{corr}$  values of the PU/PPY and PU/PNY hybrid coating increased to  $-1.06 V$  and  $-0.99 V$ , the  $I_{corr}$  values decreased to  $6.76 \times 10^{-5} A/cm^2$  and  $5.62 \times 10^{-5} A/cm^2$ . The  $E_{corr}$  values of the PU/PPN and PU/ PU/PZP hybrid coating increased to  $-0.99 V$  and  $-0.84 V$ , the  $I_{corr}$  values decreased to  $3.39 \times 10^{-5} A/cm^2$  and  $2.30 \times 10^{-5} A/cm^2$ . The  $E_{corr}$  values of the PU/PPZO hybrid coating are maximum and the  $I_{corr}$  values are minimum. From

Tab. 1, it can be seen that the  $V_{\text{corr}}$  values decreased and the  $\beta_a$  and  $\beta_c$  values increased when the steel substrate was coated. Especially, the  $V_{\text{corr}}$  values of PU/PPZO are minimum and the  $\beta_a$  and  $\beta_c$  values of PU/PPZO are relatively large. Hence, it indicated that the anticorrosive performance of PU/PPZO hybrid coating was better than that of other coatings.

From the above, the coating contained composite fillers, which improved the corrosion performance. When the steel substrate was coated with PU/PPY hybrid coating or PU/PNY hybrid coating, the passivation of the metal surface due to the formation of ferric oxide protected the underlying steel [26]. When the steel substrate was coated with PU/PPN hybrid coating, the increase of polymer monomer can enhance the compactness of molecular structure, it indicates the formation of a great barrier. For the PU/PZP hybrid coating, the addition of nano-ZnO can form the core-shell structure, which also enhances the compactness and conductivity of molecular structure. Atta [27] have confirmed that the core-shell structure of conducting polymers produces the protection of anode to protect the steel in the process of electrochemical. When PPZO was added into coating, the PU/PPZO hybrid coating presented the combined properties, so it is the most effective in the protection of underlying steel [28-29].

### 3.2.3 EIS studies



**Figure 8.** the EIS curves of (a) uncoated steel, (b) pure PU coating, the hybrid coating of (c) PU/PPY, (d) PU/PNY, (e) PU/PPN, (f) PU/PZP and (g) PU/PPZO

Fig. 8 shows the EIS curves of uncoated steel, pure PU coating, the hybrid coating of PU/PPY, PU/PNY, PU/PPN, PU/PZP and PU/PPZO in 3.5% NaCl solution for a period of time. The EIS curves of  $Z'$  refer to the real part of the impedances,  $Z''$  refers to the imaginary part of the impedances. Generally, if the semicircle of EIS curves has larger diameter, it refers to slower rate of corrosion, we can take from the diameter of the curves forming semicircle as the indicator of the anticorrosive performance [30]. From Fig. 8, it can be seen that EIS curves of all coatings show similar semicircles.

However, the diameter of EIS curves of PU/PPZO hybrid coating is the largest and the diameter of EIS curves of uncoated steel is the least, which indicates the anticorrosive performance of PU/PPZO hybrid coating is best and the uncoated steel is the worst. The diameter of EIS curves of PU/PZP hybrid coating is larger than the hybrid coating of PU/PPY, PU/PNY, and PU/PPN. Moreover, the hybrid coating of PU/PPN is better than the PU/PNY and PU/PPN hybrid coating. Thus it can be seen that the PU/PPZO hybrid coating can form not only a great barrier but also the protection of anode and the passivation of the metal surface [31-33].

### 3.2.4 Immersion test

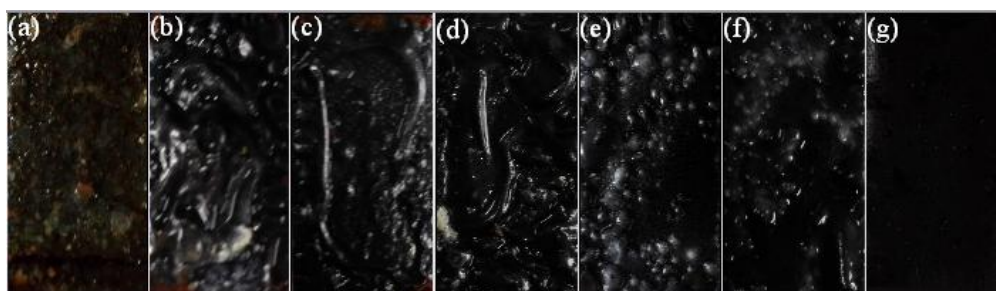


**Figure 9.** The photographs of (a) uncoated steel, (b) pure PU coating, the hybrid coating of (c) PU/PPY, (d) PU/PNY, (e) PU/PPN, (f) PU/PZP and (g) PU/PPZO after in mmmersion in 3.5% NaCl solution for 100days

To further study the actually anticorrosion performance of coating [3-4], the appearance of uncoated and coated steel after the immersion test for 80 days in 3.5% NaCl solution are showed in Fig. 9. It can be seen that the uncoated steel suffered from serious corrosion in large scale with red rust layers. The PU coating of steel was subjected to localized corrosion with red rust layers. The PU/PPY and PU/PNY hybrid coating of steel bubbled in large scale, and the PU/PPY hybrid coating appeared the red rust layers. The PU/PPN, PU/PZP hybrid coating of steel just were found a amount of small bubbles [35-39]. However, the the coating surface of the PU/PPZO hybrid coating of steel, doesn't have obvious corrosion phenomena.

## 4. CONCLUSIONS

The PPZO composite has been prepared on the surface of nano-ZnO particles using p-toluenesulfonic acid as dopant by in situ polymerization method. The SEM images show the morphology of composite, it indicates that nano-ZnO particles are homogeneous dispersed in the polymer and improve the compactness of the molecules structure. The XRD pattern explains that the polymer has no effect on crystallization performance of nano-ZnO. The UV-vis and FT-IR spectra explain the certain interaction exists between the polymer and nano-ZnO. The corrosion resistance of coating was measured by the electrochemical measurements and the immersion text in 3.5% NaCl solution, it indicates that the corrosion resistance of the PU/PZP hybrid coating was optimum. The

higher corrosion protection ability of the PU/PZP hybrid coating was due to the great barrier, the protection of anode and the passivation of the metal surface.

## References

1. C.W. Peng, K.C. Chang, C.J. Weng, M.C. Lai, *Electrochim. Acta*, 95 (2013) 192
2. Y.H. Lei, N. Sheng, *Corros. Sci.*, 76 (2013) 302
3. C.Y. Ge, X.G. Yang, B.R. Hou, *J. Coat. Technol. Res.*, 9 (2012) 59
4. J.O. Iroh, W.C. Su, *Electrochim. Acta*, 46 (2000) 15
5. G. Inzelt, M. Pineri, J.W. Schultze, M.A. Vorotyntseva, *Electrochim. Acta*, 45 (2000) 2403
6. J. Hou, G. Zhu, J.Q. Zheng, *Polym. Sci. Ser. B.*, 53 (2011) 546
7. O. Ali, R. Nosrati, *Pro. Org. Coat.*, 76(2013) 113
8. W.W. Deng, Y.F. Shena, X.M. Liang, J.W. Feng, H.X. Yang, *Electrochim. Acta*, 147 (2014) 426
9. H. Kim, W.J. Chang, *Synth. Met.*, 101 (1999) 150
10. J. Yang, M. Cho, C.H. Pang, Y.K. Lee, *Sensor. Actuat. B-Chem.*, 211 (2015) 93
11. R. Scherer, A.M. Bernardes, M.M.C. Forte, J.Z. Ferreira, C.A. Ferreira, *Mater. Chem. Phys.*, 71 (2001) 131
12. K. Qi, Y.B. Qiu, Z.Y. Chen, X.G. Guo, *Corros. Sci.*, 91 (2015) 272
13. K.R.L. Castagno, D.S. Azambuja, V. Dalmoro, *J. Appl. Electrochem.*, 39 (2009) 93
14. T. Ohtsuka, M. Iida, M. Ueda, *J. Solid State. Electrochem.*, 10 (2006) 714
15. T. Tuken, B. Yazic, M. Erbil, *Mater. Design*, 28 (2007) 208
16. B. Duran, G. Bereket, *J. Coat. Technol. Res.*, 10 (2013) 897
17. A. Mostafaei, F. Nasirpour, *Pro. Org. Coat.*, 77 (2014) 146
18. I.L. Lehr, S.B. Saidman, *Pro. Org. Coat.*, 76 (2013) 1586
19. K.R.L. Castagno, V. Dalmoro, R.S. Mauler, D.S. Azambuja, *J. Polym. Res.*, 17 (2010) 647
20. D.C. Tiwari, P. Atria, R. Sharma, *Synth. Met.*, 203 (2015) 228
21. J.C. Xu, W.M. Liu, H.L. Li, *Mat. Sci. Eng. C.*, 25 (2005) 444
22. S.K. Dhoke, A.S. Khanna, *J. Appl. Polym. Sci.*, 113 (2009) 2232
23. H. Hammache, L. Makhloufi, B. Saidani, *Corros. Sci.*, 45 (2003) 2031
24. M.G. Hosseini, M. Sabouri, T. Shahrabi, *Pro. Org. Coat.*, 60 (2007) 178
25. W.A. Badawy, K.M. Ismail, A.M. Fathib, *Electrochim. Acta*, 51 (2006) 4182
26. P. Herrasti, A.I.D. Rio, J. Recio, *Electrochim. Acta*, 52 (2007) 6496
27. A.M. Atta, O.E. El-Azabawy, H.S. Ismail, M.A. Hegazy, *Corros. Sci.*, 53 (2011) 1680
28. H.J. Adler, *Corros. Sci.*, 47 (2005) 3216
29. A.M. Fenelon, C.B. Breslin, *Electrochim. Acta*, 47 (2002) 4467
30. K.R.L. Castagno, V. Dalmoro, D.S. Azambuja, *Mater. Chem. Phys.*, 130 (2011) 721
31. T.V. Schaftinghen, C. Deslouis, A. Hubin, H. Terryn, *Electrochim. Acta*, 51 (2006) 1695
32. A.C. Balaskas, I.A. Kartsonakis, G. Kordas, A.M. Cabral, P.J. Morais, *Pro. Org. Coat.*, 71 (2011) 181
33. S.Y. Huang, P. Ganesan, B.N. Popov, *Appl. Catal. B-Environ.*, 93 (2009) 75
34. H. Duan, K. Du, C.W. Yan, F.H. Wang, *Electrochim. Acta*, 51(2006) 2898
35. Y.H. Lei, N. Sheng, A. Hyono, M. Ueda, T. Ohtsuka, *Pro. Org. Coat.*, 77 (2014) 774
36. E. Armelin, R. Pla, F. Liesa, X. Ramisc, J.I. Iribarren, C. Aleman, *Corros. Sci.*, 50 (2008) 721
37. E. Armelin, A. Meneguzzi, C.A. Ferreira, C. Aleman, *Surf. Coat. Tech.*, 203 (2009) 3763
38. A. Gergely, E. Pfeifer, I. Bertoti, T. Torok, E. Kalman, *Corros. Sci.*, 53 (2011) 3486
39. M.C. Turhan, M. Weiser, H. Jha, S. Virtanen, *Electrochim. Acta*, 56 (2011) 5347